

## Numerical analysis of a deep drawing process with additional force transmission for an extension of the process limits

This content has been downloaded from IOPscience. Please scroll down to see the full text.

2017 IOP Conf. Ser.: Mater. Sci. Eng. 179 012006

(<http://iopscience.iop.org/1757-899X/179/1/012006>)

View [the table of contents for this issue](#), or go to the [journal homepage](#) for more

Download details:

IP Address: 194.95.157.184

This content was downloaded on 25/04/2017 at 08:30

Please note that [terms and conditions apply](#).

You may also be interested in:

[A numerical analysis on forming limits during spiral and concentric single point incremental forming](#)

M L Gipiela, V Amauri, C Nikhare et al.

[Design and Analysis of Deep Drawing Process on angular Deep Drawing Dies for Different Anisotropic Materials](#)

P Venkateshwar Reddy, Perumalla Janaki Ramulu, G Sandhya Madhuri et al.

[Influence of the tool temperature increment on the coefficient of friction behavior on the deep drawing process of HSS](#)

I Gil, L Galdos, E Mugarra et al.

[Modelling of fracture effects in the sheet metal forming based on an extended FLC evaluation method in combination with fracture criterions](#)

P Hora, M Gorji and B Berisha

[A Triaxial Failure Diagram to predict the forming limit of 3D sheet metal parts subjected to multiaxial stresses](#)

F Rastellini, G Socorro, A Forgas et al.

[Development of an intelligent tool system for flexible L-bending process of metal sheets](#)

Ming Yang, Ken-ichi Manabe and Hisashi Nishimura

[Cluster compaction of two-dimension spherical particles binary mixture as model of forming process of an asteroid](#)

S Viridi and B Dermawan

# Numerical analysis of a deep drawing process with additional force transmission for an extension of the process limits

B-A Behrens<sup>1</sup>, C Bonk<sup>1</sup>, N Grbic<sup>1,2</sup>, M Vucetic<sup>1</sup>

<sup>1</sup>Institute of Forming Technology and Machines, Leibniz Universität Hannover, An der Universität 2, 30823 Garbsen

<sup>2</sup>E-mail: grbic@ifum.uni-hannover.de

**Abstract.** By sheet metal forming processes the forming limits and part characteristics are defined through the process specific loads. In deep drawing processes the maximum deep draw ratios as well as the springback behaviour of the metal parts are depending on the stress distribution in the part material during the forming process. While exceeding the load limits, a failure in the material occurs, which can be avoided by additional force transmission activated in the deep drawing process before the forming limit of material is achieved. This contribution deals with numerical investigation of process effect caused by additional force transmission regarding the extension of the process limits. Here, the steel material HCT 600X+Z (1.0941) in thickness  $s_0 = 1.0$  mm is analyzed numerically using the anisotropic model Hill48. This model is validated by the means of cup test by Swift. Both, the FEA of conventional and forming process with additional force transmission are carried out. The numerical results are compared with reference geometry of rectangle cup.

**Keywords:** deep drawing, process limit, deep drawing with additional force transmission, deep drawing with counter punch, FEA

## 1 Introduction and motivation

Increasing globalization, resulting in a rapid change of the industrial market and the society, strictly expected regulation of CO<sub>2</sub> emissions and the increasing scarcity of resources are the main drivers of the automotive industry. A great potential for decrease CO<sub>2</sub> emissions is to reduce the vehicles mass in the car body. Therefore, the continuous innovation of existing production processes are required, with the aim to develop processes with a high level of productivity, minimum number of production stages, maximum utilization of the material, low revision need, aspired energy balance and high shape or dimensional accuracy. By production of car body parts made from sheet metals, the deep drawing and bending are crucial. In order to expend the process limits by sheet metal forming, the development of innovative processes is required. Here, the finite element method is an indispensable tool.

## 2 State of the art

By sheet metal forming processes the force, applied in sheet metal, causes the modification of its geometry without removing any material. The stresses distributed over the metal part are beyond the yield strength of material inducing the plastic deformation in sheet metal without material failure.

As extensively used sheet metal forming process the deep drawing is applied in the production of different metal parts like pots and pans for cooking, containers, sinks, automobile parts, such as panels and gas tanks.



## 2.1 Conventional deep drawing

Conventional deep drawing is a sheet metal forming process which requires a blank, blank holder, punch, and draw ring (die) (see Figure 1). Here, the blank as a piece of sheet metal is radially drawn or stretched into the desired shape by the means of specific force transmission induced from the mechanical punch load. The important area of the punch is the radius, where the forming load is transferred through the drawn part wall into the deformation zone (flange). During the conventional deep drawing process the blank is clamped by the blank holder above the die. The external shape of the part is defined through the die cavity. The cross section of the drawn part can pass different shapes, with straight, tapered, or even curved walls. Here, the cylindrical or rectangular parts are most common.

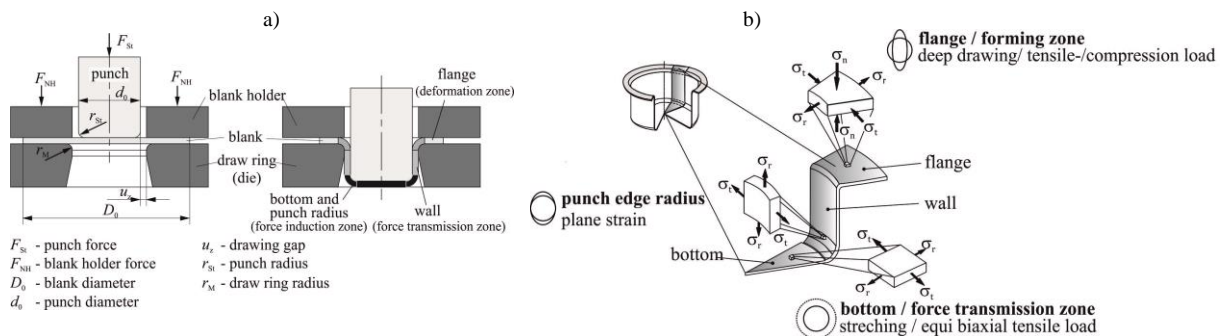


**Figure 1.** Conventional deep drawing a) positioning and forming, b) stress distribution.

Due to tensile forces effecting part wall, blank thinning is occurring. Based on the local stresses an uneven wall thinning appears. At the punch radius where the part wall loses contact with the punch, the part wall thickness shows lowest value. Here, the part failure can occur. Thus, the maximum stress, which can be transferred to the deformation zone (flange) is determined [1].

## 2.2 Deep drawing with additional force transmission

For extension of forming limits deep drawing processes are applied like hydro-mechanical deep drawing, hydro-form process or hydraulic deep drawing process [2]. The main commonality of these processes is the usage of active media for additional force transmission, by which the initial forming zone with the highest local stresses is reloaded. Thus, the additional forming load is transferred into the crucial deformation zone (flange). Hereby, a further material drawing can occur.

The extension of forming limits can be also achieved by the means of additional mechanical force transmission. Here, between different process approaches can be distinguished like additional material feeding [3], usage of differentiated force transmission through the variable surface pressure in the blank holder or counter-punch, as well as by an expansion punch.

By additional material feeding the crucial tensile stresses can be decreased when pulling the material in the flange area by additional mechanical load. Thus the punch force transmission is reloaded. Other approaches deal with specific adjustment of friction. Due to the reduction of the friction at draw ring radius a further material drawing from the flange area is realized. By processes with defined material flow a cup is first drawn and subsequently the material is pushed over the wall by means of a mechanical load, while the drawing punch transforms the metal part.

The usage of differentiated force transmission through the variable surface pressure in the blank holder allows the reduction of the friction between blank holder and die. Thus, the material flow is supported by deep drawing process. Here, by means of stiffness-optimized blank holder systems the local surface pressure in the flange area can be varied and suited for better process stability.

By differentiated force transmission using the expansion punch the force transmission takes place at whole lateral surface of the part wall. Here, the distribution of the forming load at part wall occurs by using a specific punch with grub-screw grooves, which are machined for force application into the inner part wall [2, 3].

### 2.3 New tool system developed for deep drawing with additional mechanical force transmission

The new tool system designed for deep drawing process with additional mechanical force transmission is developed at Institute of Forming Technology and Machines (Figure 2a). At punch radius and the transfer zone to the wall area, where the highest stretching of material occurs, the forming load is transmitted into the flange zone (forming zone) by the means of external pressure applied on the part bottom (see Figure 2b).

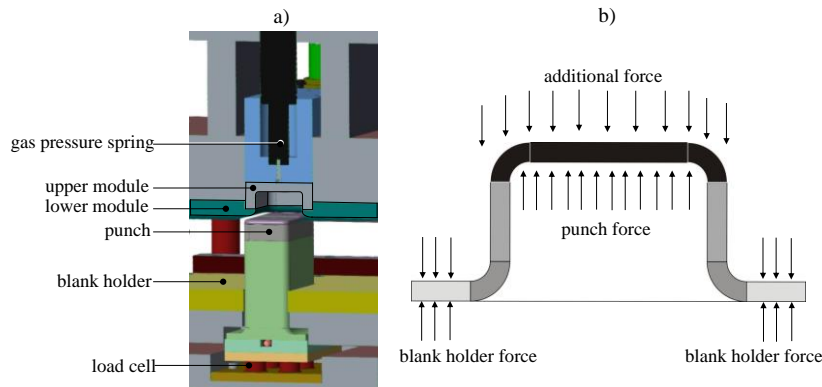


**Figure 2.** Additional force transmission, a) tool system, b) schematic description.

The punch is located on the base plate and the load cells are placed between. The blank holder device is mounted on an intermediate plate with guiding elements, which is located on the top of press quills. Thus, the deep drawing takes place in return. The closed die is designed as two-part module, the upper and lower die module. The lower die module, or the drawing ring, represents the rectangle cup. The upper die module represents the geometrical shape of the drawing part bottom. Here, besides the force in the part bottom also the force in radius between bottom and wall of the drawn part is transferred by the upper die module which works like a counter punch. This is initiated when the drawn part runs into the upper die, whereby a vertical additional force in the drawing process from bottom into the flange zone is transferred by means of a gas pressure spring. The gas spring is fixed to the counter punch.

## 3 Numerical Analysis

By FEA of the effect caused by the additional force transmission, the processes with and without the activation of the gas pressure spring were taken into account. For numerical investigation the rectangle cup part made of steel material HCT 600X+Z100 in thickness of  $s_0 = 1.0$  mm is chosen.

### 3.1 Material modelling

For modelling of material behavior flow criterion by Hill [4] is used in Abaqus. Based on six material-specific coefficients calculated from anisotropic coefficients (r-values) the shape of the yield locus is generated. Here, quasi-static uniaxial tensile tests were performed and analyzed according to DIN EN ISO 10002. The specimens aligned at  $0^\circ$ ,  $45^\circ$  and  $90^\circ$  to the rolling direction were tested at room temperature. Thus, the r-values  $r_0$ ,  $r_{45}$  and  $r_{90}$  are determined.

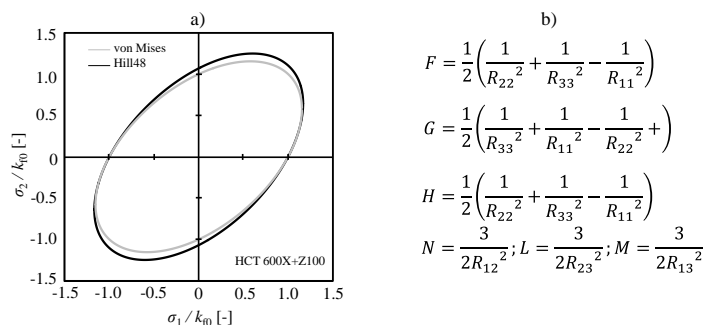


**Figure 3.** Material modelling by Hill48 for HCT600 a) yield locus b) Hill-coefficients.

In Figure 3 the yield locus according to Hill48 and von Mises for material HCT 600 is presented. For further investigations the yield locus modeled by Hill48 is used. For parametrization of the Hill criterion in Abaqus, a calculation of Abaqus-suited Hill coefficients is carried out (see Table 1).

**Table 1.** Parametrization of Hill material model for HCT 600

HCT600	$r_0$	$r_{45}$	$r_{90}$	$G$	$H$	$F$	$N$	$L$	$M$	$R_{11}$	$R_{22}$	$R_{33}$	$R_{12}$	$R_{13}$	$R_{23}$
[-]	0.932	1.042	1.197	0.5457	0.454	0.387	1.662	3/2	3/2	1.0	1.067	1.049	1.034	1.0	1.0

Beyond the point of uniform elongation the true stress - true plastic strain curve determined in the uniaxial tensile test needs to be extrapolated for the FEA. By material modelling with the extrapolation process an inaccurate description of the material behavior at high strain can occur. Thus, the steel material HCT 600 was analyzed in a hydraulic bulge test [5].

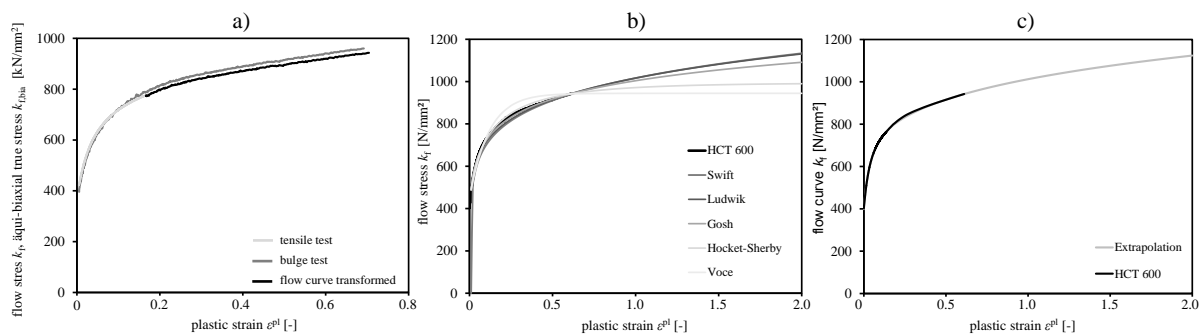


**Figure 4.** HCT 600  $s_0=1.0$  mm a) experimental results, b) extrapolation, c) best-fit extrapolation. The biaxial true stress - true plastic strain curve from the bulge test is transformed to the uniaxial stress state with a mathematical approach based on the principle of the equivalence of plastic work (Figure 4a) [6]. Thus, more experimental data can be taken into account for the following extrapolation process (Figure 4b). Here, the deviation from the actual flow behaviour at high strains made by the extrapolation is minimized.

The extrapolation functions presented in Figure 4b) can not correctly reproduce the flow behavior of the experimentally determined flow curve for the HCT 600. In order to achieve an accurate description of the hardening behavior at high plastic strains a combined approach based on Swift and Hockett-Sherby is used (see Figure 4c) [7]:

$$k_f = \alpha_s \cdot (A_s \cdot (B_s + \varphi_{pl})^{n_s}) + (1 - \alpha_s) \cdot (A_{HS} - (A_{HS} - B_{HS})e^{-C_{HS}\varphi_{pl}^{n_{HS}}}) \quad (1)$$

The extrapolation coefficients for the combined extrapolation functions by Swift and Hockett-Sherby are summarized in Table 2.

**Table 2.** Coefficients related to Swift / Hockett-Sherby combined approach for HCT 600

Swift / Hockett-Sherby	$\alpha_s$	$A_s$	$B_s$	$n_s$	$B_{HS}$	$A_{HS}$	$C_{HS}$	$n_{HS}$
[-]	0.42	1800	0.01218	0.2	147.3	438.9	21.59	0.9397

### 3.2 Model validation

Using the cup test by Swift the material modelling approach Hill48 is validated quantitatively. The test is carried out on universal Roell+Korthaus machine, while the force and displacement are measured. Afterwards, the forming process based on Swift is analyzed numerically with the software Abaqus CAE 6.13-1 (Figure 5a). Here, the values force and displacement are calculated and compared with experimental results. The reaction forces of both, the test and the FEA, are showing a typical evaluation for a deep drawing process. Here, the punch forces determined by the experiments show a good agreement with the numerical results (Figure 5b). For further verification of the Hill model the geometry of the cup is measured optically with ATOS system (GOM mbH). Here, the experimentally

and numerically determined CAD geometries of a round cup are compared digitally with software Geomagic® Qualify™ (Geomagic, USA) (see Figure 5c).

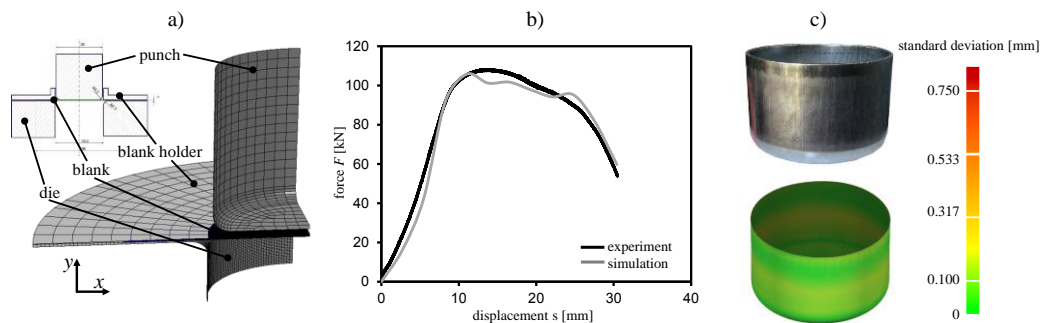


**Figure 5.** Quantitative model verification, a) FE model cup test by Swift b) comparison force-displacement curve, c) geometric comparison.

Two geometries, CAD from experiment and CAD from FEA, are aligned with each other and the best fit analysis of dimensional matching between the experimental and numerical results is carried out. For this analysis, the optically measured geometry is chosen as a reference. The dimensional deviation analysis shows a standard deviation of 0.089 mm regarding the whole dimensional deviation. The presented results show a sufficient agreement between the FE results and the real part. Hence, the material model by Hill48 will be used for the further numerical process analysis.

### 3.3 FEA of deep drawing process with additional force transmission

In order to investigate the effect caused by additional force transmission the FEA of deep drawing process, presented in section 2.3, is carried out. Hereby, both processes, the conventional process and process with additional force transmission are investigated numerically (see Figure 6a,b).

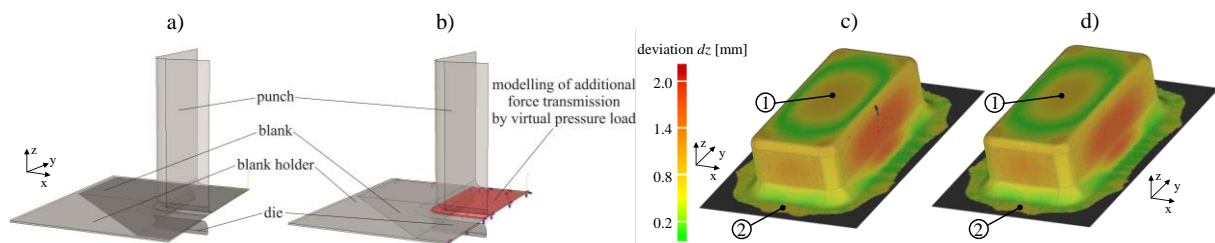


**Figure 6.** HCT 600, a) FE model conventional process, b) FE model deep drawing with additional force transmission, c) comparison of FEA results (conventional deep drawing) with reference CAD-geometry, d) comparison of FEA results (process with additional force transmission) with reference CAD-geometry

For 3D FE modelling, consisting of punch, die, blank holder and blank, a quarter model is applied. Here, the Hill48 model with the isotropic hardening rule is used. Based on calculation of effective E-modulus using the exponential approach by Yoshida [8] the springback behaviour is calculated with Abaqus/Standard implicit solver. The interaction between blank and active surface of the tool system is modelled with Coulomb's friction model. For FEA of deep drawing with additional force transmission the 3D FE model of conventional process (Figure 6a) is extended with a virtual pressure component (see Figure 6b). The numerical results are compared with reference CAD-geometry of the rectangle cup part (see Figure 6c,d). The positions 1 and 2 of the cup parts are considered for geometric 2D-comparison (Figure 7).

The corresponding positions of reference CAD-geometry and CAD from FEA are matched with each other and the best fit analysis of dimensional 2D-matching is carried out using the software Geomagic® Qualify™. Regarding the bottom area (position 1) the dimensional deviation analysis shows a positive deviation of  $dz = 1.186$  mm for conventional deep drawing and  $dz = 0.113$  mm by process with additional force transmission, which means a geometrical improvement of the rectangle cup by 6.16% regarding the part bottom area.

Furthermore, a negative deviations of  $dz = -0.345$  mm by conventional deep drawing and of  $dz = -0.294$  mm by process with additional force transmission, in the flange area (position 2) are determined. This corresponds into a reduction of the flange springback by 14.78 %.

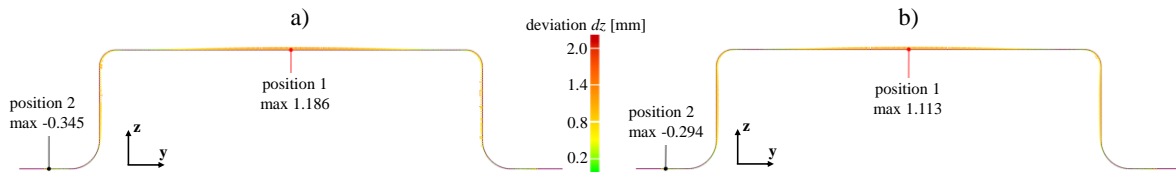


**Figure 7.** Geometric 2D-comparison, a) conventional process / reference CAD-geometry, b) process with additional force transmission / reference CAD-geometry,

Due to the activation of the additional force transmission, in the bottom area of the rectangle cup part, the effect of the reduction of the springback in the flange area is verified numerically. Based on numerical results an improved shaping of the bottom of the rectangle cup part can be expected by the means of additional force transmission.

#### 4 Summary and Outlook

In order to expand the process limits by deep drawing, the development of innovative processes using the FEA is required. In earlier process design phase the tool system is developed, which allows the activation of additional force transmission in the bottom area of the drawn rectangle cup part with a counter punch. The deep drawing process with additional force transmission is investigated numerically. Here, the validated material model Hill48, based on anisotropic coefficient for describing the anisotropic material behaviour, is used. By the means of FEA a positive effect of additional force transmission, resulting in reduction of the springback in the flange area and improvement of shaping in the bottom of the rectangle cup part, can be determined numerically.

In next research step experimental investigations on the new tool system are planned. For model verification the comparison between numerical and experimental results will be carried out.

#### Acknowledgement

This paper is based on investigations of the project (BE169/139-1): “*Deep drawing with additional force transmission*”, which is kindly supported by the German Research Foundation (DFG). The authors thank the DFG for project foundation.

#### References

- [1] Doege E and Behrens B-A 2010 Handbuch der Umformtechnik, Springer ISBN 978-3-642-04248-5
- [2] Siebel E 1953 WERKSTOFFMECHANIK, VDI-Sonderheft Werkstoffe I, VDI-Verlag Düsseldorf
- [3] Otto M 2003 Erweiterung der Umformgrenzen beim Tiefziehen und Kragenziehen durch Nachschieben von Werkstoff, Dissertation, Universität Magdeburg
- [4] Hill R 1948 A theory of the yielding and plastic flow of anisotropic metals, Proceedings of the Royal Society of London, Series A., Vol. **193**, 281-197.
- [5] Hallfeldt T, Hotz W, Leppin, C, Keller S, Friebe H, Till E T, Müller R, Vučetić M and Vegter H 2014 Sheet Bulge Testing, Book Chapter in Comprehensive Materials Processing Volume **1** May 2014, Pages 85-93, ISBN: 978-008096533-8, Elsevier Ltd.
- [6] Sigvant M, Mattiasson K, Vegter H and Thilderkvist P 2009 A viscous pressure bulge test for the determination of a plastic hardening curve and equibiaxial material data, original research, Springer, DOI 10.1007/s12289-009-0407-y
- [7] Behrens B-A, Bouguecha A, Vucetic M and Peshekhodov I 2012 Characterisation of the quasi-static flow and fracture behaviour of dual-phase steel sheets in a wide range of plane stress states, in Archives of Civil and Mechanical Engineering **12** (4), pp. 397-406
- [8] F. Yoshida, T. Uemori, “A model of large-strain cyclic plasticity describing the Bauschinger effect and workhardening stagnation”, International Journal of Plasticity, PII S0749-6419(01)00050-X, 2001